

COMMSCOPE®



# Beamformers Explained

Dr. Mohamed Nadder Hamdy, PhD.

## Table of Contents

|   |    |
|---|----|
| <b>The rise of beamformers</b> .....                  | 2  |
| <b>Chapter 1: Beam management procedures</b> .....    | 3  |
| Idle mode beam management .....                       | 3  |
| Synchronization signals .....                         | 3  |
| Initial access .....                                  | 4  |
| Connected mode beam management .....                  | 5  |
| Reference signals .....                               | 5  |
| Connected mode procedures .....                       | 6  |
| <b>Chapter 2: Beamformers basics</b> .....            | 8  |
| Phased arrays beamforming .....                       | 8  |
| Antenna elements .....                                | 8  |
| Antenna array patterns .....                          | 8  |
| Analog and digital beamforming .....                  | 11 |
| Analog beamforming .....                              | 11 |
| Digital beamforming .....                             | 12 |
| Hybrid beamforming .....                              | 12 |
| <b>Chapter 3: Building a passive beamformer</b> ..... | 12 |
| Adaptive array antennas (AAA) .....                   | 12 |
| Planar arrays .....                                   | 12 |
| Column pattern and mutual coupling .....              | 13 |
| Scanning angle limitations .....                      | 14 |
| Radiating patterns .....                              | 14 |
| Supporting radios .....                               | 16 |
| Antenna parameters settings .....                     | 16 |
| Calibration port .....                                | 17 |
| Example: Practical Implementation with the AAA .....  | 18 |
| <b>Chapter 4: Building a digital beamformer</b> ..... | 19 |
| Massive MIMO .....                                    | 19 |
| Massive MIMO dimensioning .....                       | 19 |
| Beamforming type .....                                | 20 |
| Antenna elements numbers .....                        | 20 |
| Transceivers numbers and mapping options .....        | 22 |
| 64T64R AE Mapping Simulation .....                    | 23 |
| <b>References</b> .....                               | 26 |

## Abstract

Beamforming antennas are an essential tool for mobile operators as they build out their networks for capacity and 5G NR. For radio planners tasked with developing 5G and capacity build-out strategies, it is critical to have a full understanding of beamforming antenna capabilities, including the variations and appropriate use cases for each type. Without this understanding, planners risk over- or under-engineering parts of their networks, resulting in unnecessary costs, insufficient performance, or both.

This paper introduces the principles of beamforming, including passive and active beamforming, different configurations and their underlying technologies. A follow-up paper, “Beamformers Explained II,” will focus on various actual applications that provide planners a methodology for selecting the right antenna for each situation.

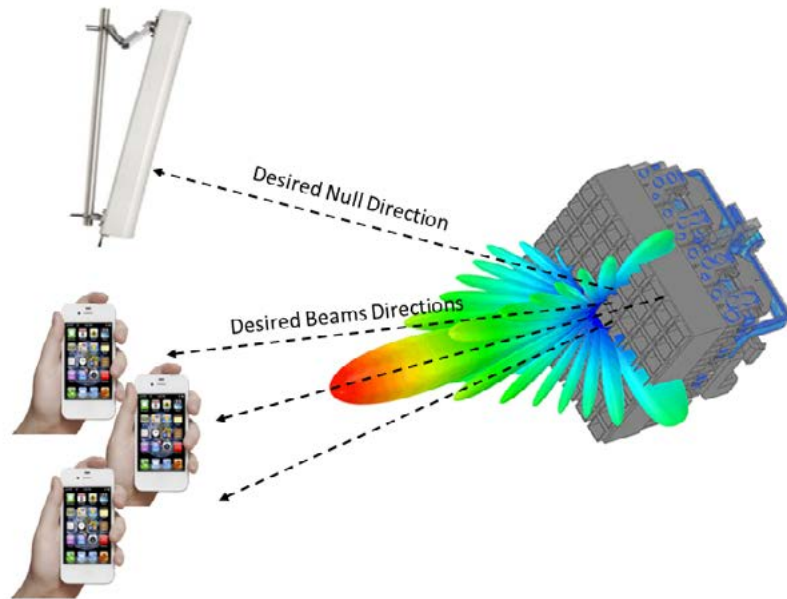
## The rise of beamformers

Unlike traditional antennas that could transmit and receive only on fixed radiation patterns, beamforming antennas dynamically shape their main and null beam directions according to the location of their connected users. Thus, these future-enabling antennas are often referred to as “beamformers.” Beamforming antennas are unique in their ability to effectively reduce interference, improve the signal-to-interference-and-noise ratio (SINR) and deliver a significantly better end user experience. With the ITU-WRC\* adoption of new sub 6 GHz and mmWave frequency bands, and the trend toward extreme spectral efficiencies used in 5G NR†, beamformers are becoming an essential weapon in the mobile operator’s arsenal.

**Beamformers offer various configurations and capabilities; each is best suited for a certain environment. Physically, these antennas might look very dissimilar, but all beamformers share three main design philosophies:**

- They contain active or passive array structures.
- They use digital, analog or hybrid beamforming.
- They are equipped with multiple radio transceivers—8T8R and higher.

\*World Radio Conference  
†5G new radio



## Chapter 1: Beam management procedures

To understand the operational aspects of beamformers, start with a functional description. The 5G NR specifications include new physical (PHY) and medium access control (MAC) layer procedures to support directional communications. Using 3GPP terminology, these procedures are referred to as **beam management**; they include four distinct operations [1].

1. **Beam sweeping:** The radiating pattern covers a spatial area, using a multi-directional beam sweep and pre-specified time intervals
2. **Beam measurement:** Evaluation of the quality of the received signal at the 5G NodeB (gNB) or the user equipment (UE)
3. **Beam determination:** Selection of the suitable beam(s), either at the gNB or the UE
4. **Beam reporting:** UE feedback on beam quality and decision information to the radio access network (RAN)

### Idle mode beam management

It is essential for the UE to establish a directional physical link connection, with its initial access (IA) to the network. Here the downlink (DL) synchronization signals play an important role.

### Synchronization signals (SS)

Unlike LTE, 3GPP defines a directional version of synchronization signals for 5G NR. This plays an important role in beam management.

**Synchronization signals** PSS, SSS, and PBCH are sent over **SS blocks**, which in turn are embedded inside larger **SS bursts** (Figure 1). Each SS block in a burst is mapped to a certain angular direction. By sequentially sweeping different angular directions, a gNB<sup>†</sup> covers a whole cell sector.

<sup>†</sup> gNB or gNodeB is the 5G NR base transceiver station

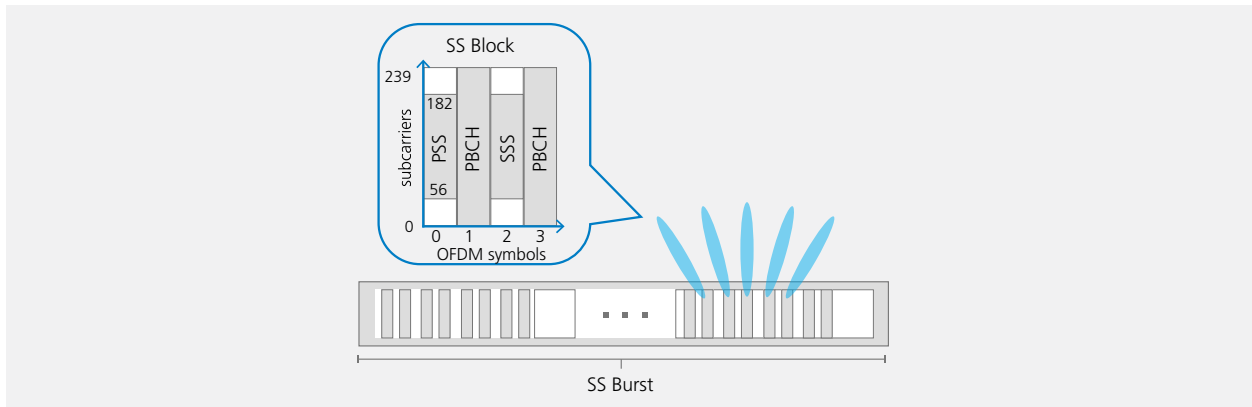


Figure 1: Directional SS blocks transmission

## Initial access

As illustrated in Figure 2, the gNB sweeps several SS blocks in different beam directions. Using beam measurement and beam determination, the UE device first evaluates and then selects the beam with the maximum signal-to-noise ratio or SNR.

The fourth key procedure, beam reporting, occurs in one of two ways:

- **Non-standalone mode (NSA)**

The UE uses the anchoring LTE connection to report the optimal set of directions to the gNBs. The gNB then schedules an immediate random access opportunity (to determine the first available resource the UE can use to transmit without colliding with other devices) for the determined direction with the full beamforming gain [2].

- **Standalone mode (SA)**

Here, without the anchoring LTE connection, the UE waits for its gNB to schedule a random access channel (RACH) opportunity. Then, the gNB in each SS block specifies one or more RACH opportunities with a certain time and frequency offset and direction. This tells the UE when to transmit its RACH preamble toward the direction as determined by the gNB.

The standalone beam reporting process may require an additional complete directional scan of the gNB for SS block transmission. This further increases the time needed to access the network.

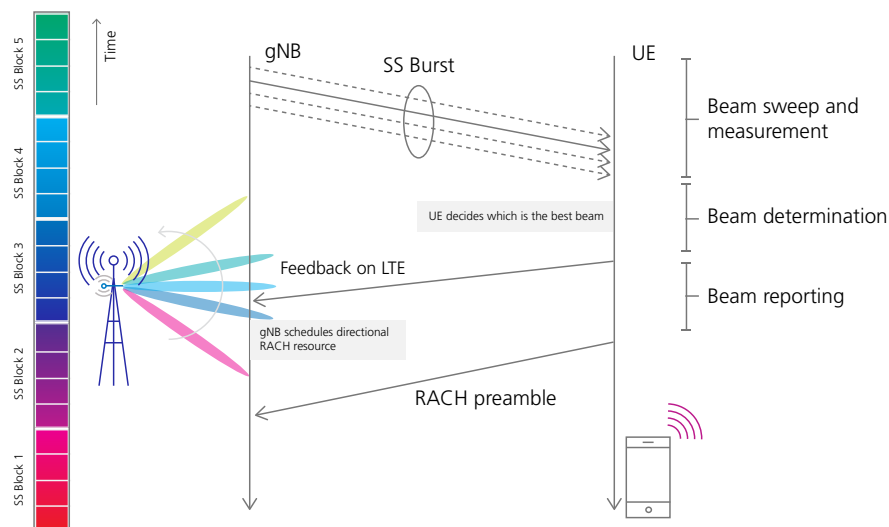


Figure 2: Initial access in NSA mode [3]

## Connected mode beam management

In connected mode, beam management is required to maintain the alignment of the transmitter and receiver beams as the UEs move—an operation defined as **tracking** [2]. Connected mode beam management uses the DL **CSI-RS** and uplink (UL) **SRS**, as will be explained.

## Reference signals

### DL channel state information reference signal

Channel state information (**CSI**) is a mechanism by which a UE utilizes a set of **reference signals** to measure and report back on channel conditions. 3GPP Rel8 and Rel9 only supported cell-specific reference signals (**C-RS**), which are utilized for both channel measurements and data demodulation. However, because the C-RS is cell based and not beam or UE specific, it causes excessive signaling overhead when operating in higher MIMO layers and beamforming modes.

**The introduction of TM9 in 3GPP Rel10** segregated the reference signals; specifically, the channel state information reference signals (**CSI-RS**) and demodulation reference signals (**DMRS**). The segregation enables the decoupling of channel measurement and data demodulation processes.

Figure 3 shows two different scenarios for handling reference signals. On the left is a cell-specific example, in which different sets of CSI signals are combined and transmitted to UEs sharing a common beam direction as per 3GPP Rel8 and Rel9. On the right is a user-specific scenario that takes advantage of TM9 in 3GPP Rel10. Here, both demodulation signals and user data are transmitted, with user data available on demand [4].

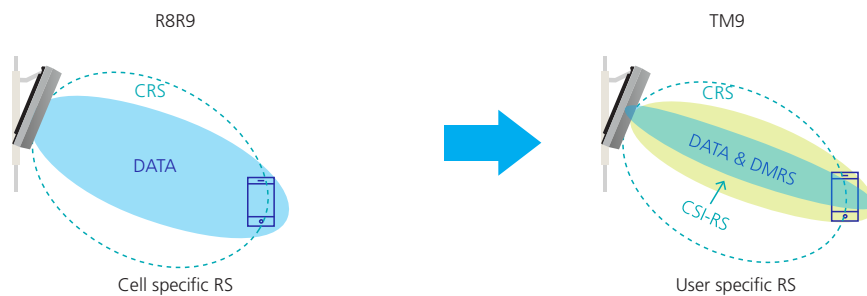


Figure 3: Cell- and user-specific RS [4]

To determine the **CSI-RS** allocation, the UE synchronizes with a given cell using the **SS bursts**, then searches for **CSI-RS** resources [5] with specified frequency and time offsets (Figure 4).

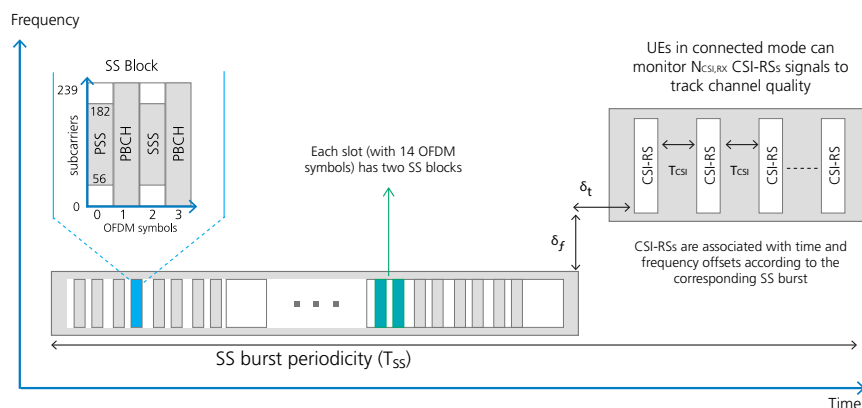


Figure 4: CSI-RS allocation [2]

## UL sounding reference signal

The UE transmits the UL sounding reference signal (**SRS**), which is used to monitor the uplink channel quality. SRS transmission is scheduled by the gNB, which also signals the UE with the resource and direction for transmitting its SRS. The UE may be configured with multiple SRSs for beam management. [5]

| Initial access (idle UE) |   | Tracking (connected UE) |
|--------------------------|---|-------------------------|
| Downlink                 | SS blocks (carrying the PSS, the SSS, and the PBCH) | CSI-RSs and SS blocks   |
| Uplink                   | 3GPP does not use uplink signals for initial access | SRSs                    |

Table 1: Reference signals for beam management operations [5]

## Connected mode procedures

Now, with the measurements' mechanisms defined, the 3GPP has further suggested three DL L1/L2 beam management procedures, commonly known as P-1, P-2 and P-3 [1]. These are a set of beam management processes to enable the UE to better receive the downlink beam (data) while in a connected state. These procedures instruct the UE to enable certain TRP<sup>§</sup> beam measurements, for selection and refinement. The concept is similar to the UE measurements triggering events, necessary for handovers and cell reselection. However, here it is meant to keep the optimal beam selected, as the UE roams across the RAN.

### P-1 (DL Tx beam and DL Rx beam selection):

#### Function:

Triggers UE measurement of TRP Tx beams for

- Selection of TRP Tx beams (TRP beamforming case)
- Selection of UE Rx beam(s) (UE beamforming case)

#### Measurements scope

- Larger, and possibly wider, set of beams
- Intra- and inter-TRP Tx beam sweep from a set of different beams

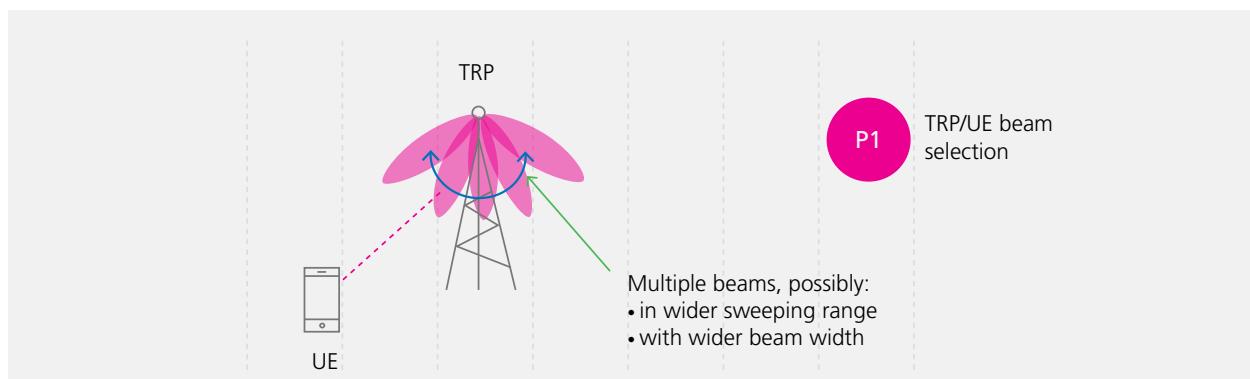


Figure 5: DL Tx beam selection [6]

§ A transmission reception point (TRxP) is defined as an antenna array, with one or more antenna elements, available to the network located at a specific geographical location for a specific area.

## P-2 (DL Tx beam refinement):

### Function

- Triggers UE measurement for TRP Tx beam refinement
- Possibly change inter/intra-TRP Tx beam(s)

### Measurements scope

- Smaller, and possibly narrower, set of TRP Tx beams than P-1

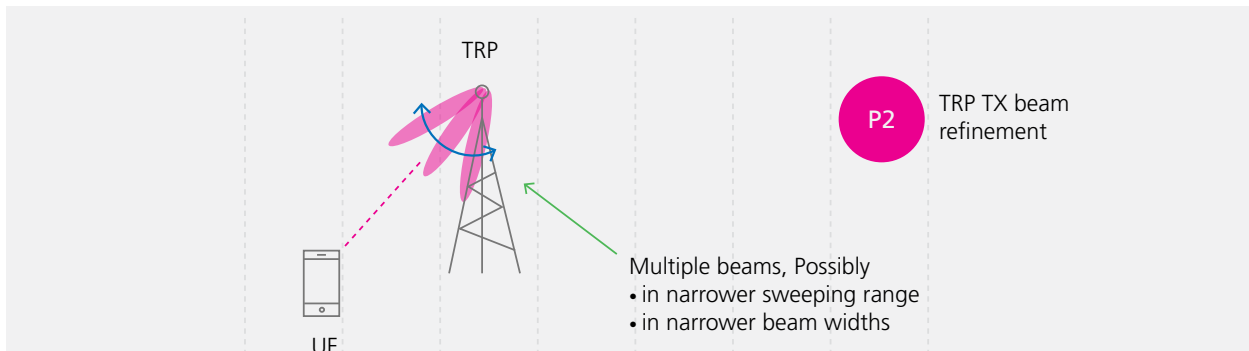


Figure 6: DL Tx beam refinement [6]

## P-3 (DL Rx beam refinement):

### Function

- Triggers UE measurement for **UE Rx beam change** (UE beamforming case)

### Measurements scope

- Same TRP Tx beam, sweeping UE Rx beam

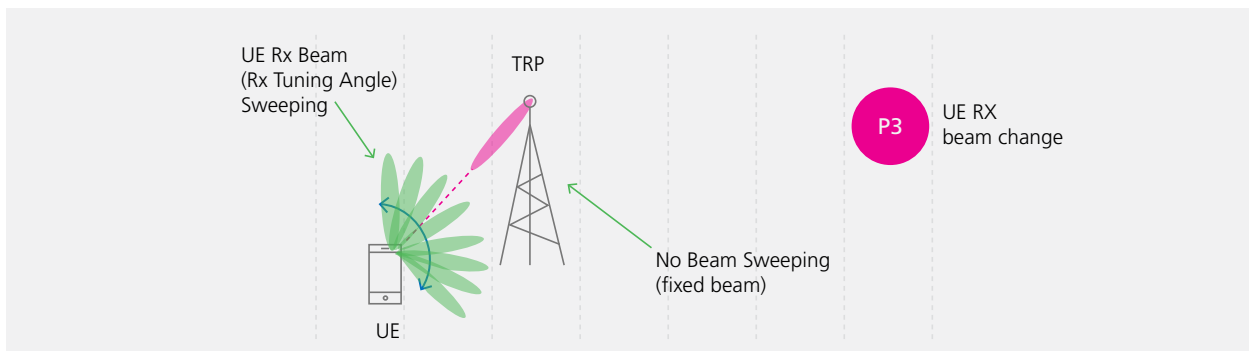


Figure 7: DL Rx beam refinement [6]

## Beam tracking

3GPP specifies that, at minimum, network-triggered aperiodic beam reporting must be supported under P-1, P-2, and P-3 operations.

A UE can also trigger mechanisms to recover from beam failure. The network explicitly configures the UE with resources for UL signal transmission for recovery purposes. The UL transmission/resources needed to report beam failure can be located in the same time instance as PRACH, or at a UE-configurable time instance. Transmission of a DL signal is supported, allowing the UE to monitor the beams and identify new potential beams.

## Chapter 2: Beamformer basics

Advanced antennas are the engines that enable beamforming capabilities. To better understand how they work, consider some of their underlying fundamental technologies.

### Phased arrays beamforming

When multiple antenna elements (AE) are mounted in a line along a shared reflector, the result is a panel antenna with linear arrays (Figure 8). A phased array antenna applies phase control (or time-delay) at each radiating element, so its beam can be shaped and scanned to different directions in space.



Figure 8: Panel antenna linear array

### Antenna elements

There are different types of AEs, with wire and aperture elements being the most common. Examples of wire AEs include dipole and monopole elements, while aperture AEs include slot elements. Some designs incorporate combinations of both types and can also be built on printed circuit boards or microstrip patches. Some examples can be seen in Figure 9.

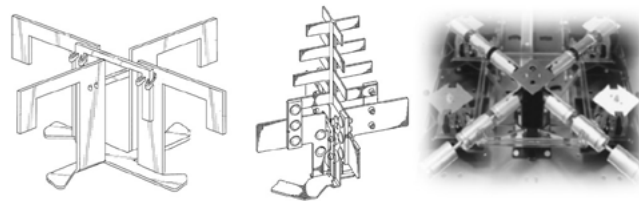


Figure 9: CommScope patented antenna element examples

Every AE has a radiation pattern, usually referred to as an **element pattern**. Specific element pattern characteristics, such as gain, are determined by the design of the element.

### Antenna array patterns

While each AE in a linear array has its own radiation pattern, the RF effect of the entire array depends on the:

- Array size and element spacing
- Elements' signal phase shifts and amplitude variation

Together, these variables describe the array factor pattern. Combining the array factor pattern and the element pattern produces the overall far field radiation pattern of the panel antenna.

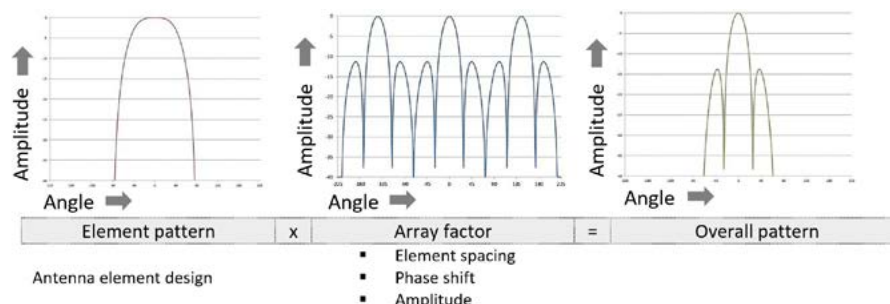


Figure 10: Array factor

## Array size effect

A uniform array with half-wavelength element spacing provides maximum directivity, which is equal to the number of array elements (N) [7]. In a lossless array, the antenna gain is equal to its directivity. This can be expressed as:

$$\begin{aligned} \text{Antenna gain (dB)} &= \text{Element gain} + 10 \log_{10}(N) \\ \text{or} &= \text{Element gain} + 3 \log_2(N) \end{aligned}$$

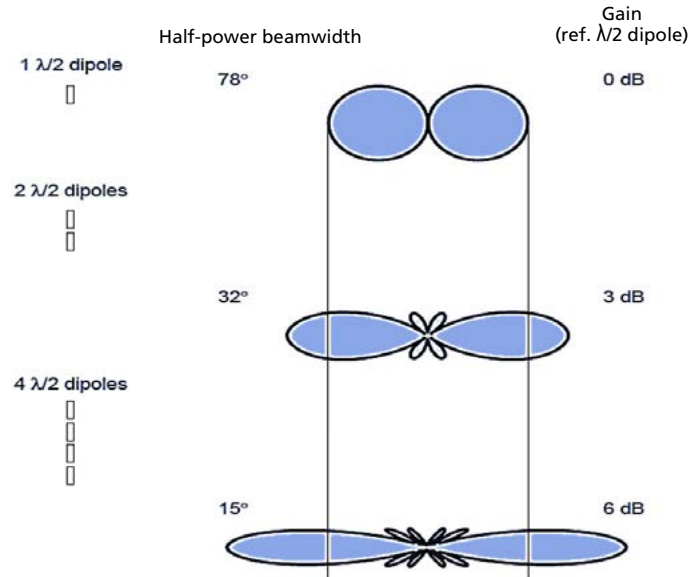


Figure 11: Relationship between number of AEs and gain

In other words, doubling (N) doubles the gain in 3 dB increments. This concept is illustrated by Figure 11, which shows the effect over the pattern's gain and V-HPBW\*\*.

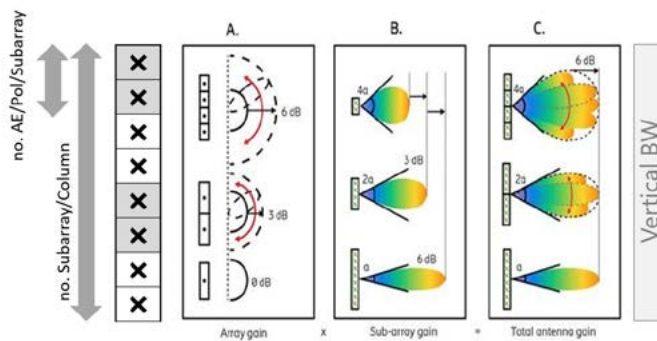


Figure 12: Subarrays gain, modified from [8]

In some designs, such as that shown in Figure 12, a linear phased array might be composed of smaller subarrays. Each subarray is connected to a different radio transceiver. The relationship between the gain of the subarray and the gain of the element can be expressed as:

$$\begin{aligned} \text{GainSubarray} &= \text{Gainelement} + 3 \log_2(N_{\text{AE/Pol./Subarray}}) \\ \text{GainArray} &= \text{GainSubarray} + 3 \log_2(N_{\text{Subarrays}}) \end{aligned}$$

\*\* Vertical half-power beamwidth

## Element spacing effect

The antenna element spacing also plays an important role in determining the pattern's shape and gain. For example, increasing the spacing for a four-element array, from  $0.5\lambda$  to  $2\lambda$ , reduces the vertical half-power beamwidth (V-HPBW) and increases the main lobe gain (Figure 13). However, this also generates more grating lobes (sidelobes), which disperse the radiated power away from the main lobe.

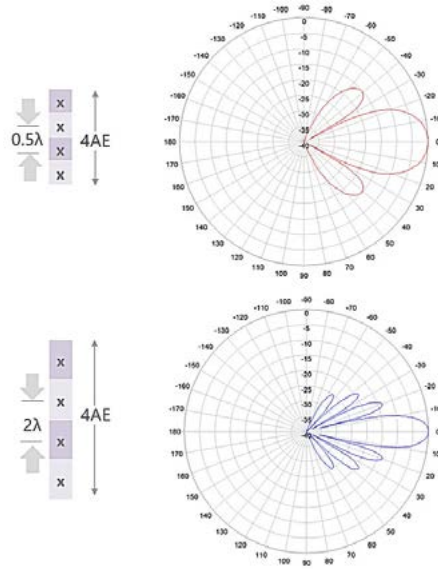


Figure 13: Antenna elements spacing effect

## Phase shift effect

In the phased array examples given thus far, it is assumed that the number of antenna elements and their spacing are fixed for each antenna. However, by controlling the RF signal phases and amplitudes feeding these AEs, it is possible to dynamically shape the array factor and the overall radiated pattern. This is the first step in building a beamformer.

It is well known that in-phase waves add up “constructively,” while out-of-phase waves diminish “destructively.” This same concept applies to RF signals. Figure 14 shows several independent analog phase shifters, placed between the radio and the antenna elements. By tuning these shifters, we can alter the pattern shape and direction.

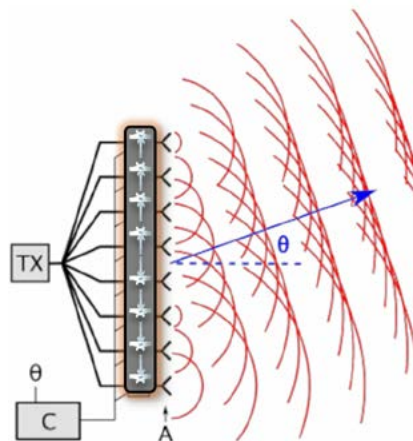


Figure 14: Effect of phase shift

## Electrical downtilting

Electrical downtilt was one of the earliest beamforming techniques used to control vertical patterns. It has since become a standard feature in almost all base station antennas (BSA).

The antenna's "electrical" downtilt is actually accomplished mechanically, as the phase shifters are adjusted either manually on the antenna itself or remotely using a controlled stepper dc motor. Figure 15 shows a dual-polarized antenna with electrical tilt and the feed network connecting the phase shifters to the AEs.

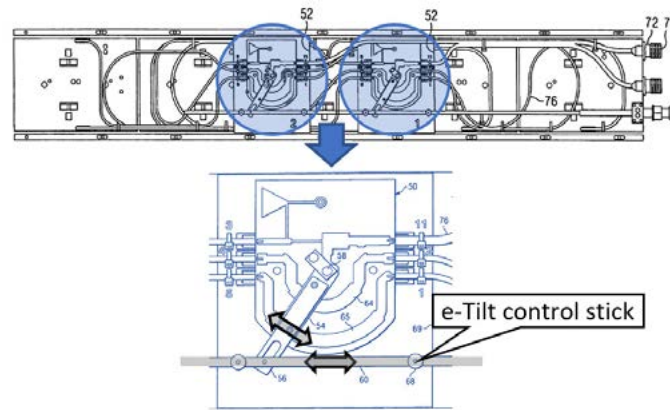


Figure 15: CommScope patented e-tilt phase shifters

## Analog and digital beamforming

Beamforming techniques can be grouped into three categories: **analog**, **digital** and **hybrid**.

### Analog beamforming

Analog beamforming, such as that shown in Figure 16, uses a single common RF source split among multiple antenna elements. The beam is controlled by adjusting analog phase shifters along the RF path. This is similar to the phased-array electrical downtilt discussed earlier.

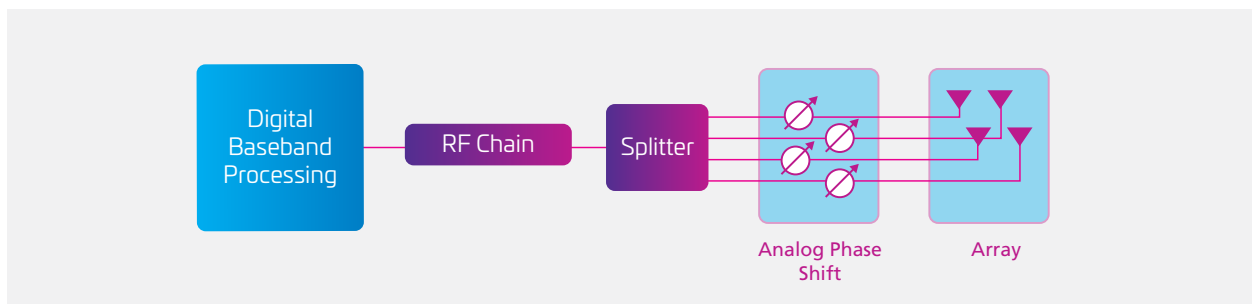


Figure 16: Analog beamforming

## Digital beamforming

In digital beamforming (Figure 17), each antenna has a dedicated RF signal and path. Phases and amplitudes are digitally controlled by baseband processing. Digital beamforming provides the best beam control; however, it suffers high power consumption and signaling overheads.

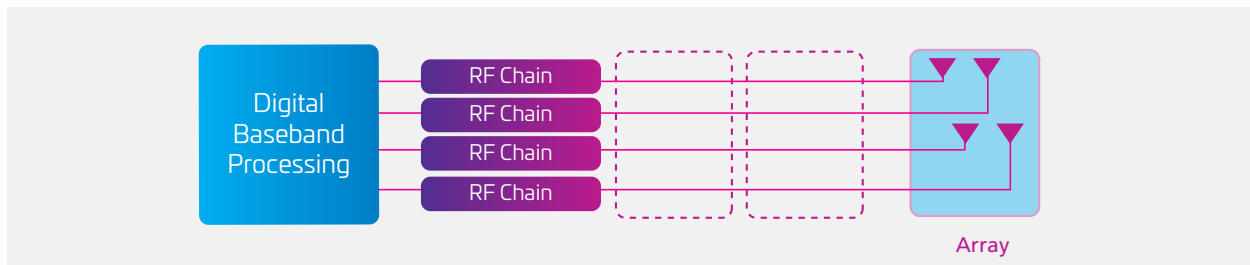


Figure 17: Digital beamforming

## Hybrid beamforming

As the name implies, a hybrid beamformer (Figure 18) combines aspects of analog and digital beamforming. It features digitally controlled RF chains, splitters and analog phase shifters.

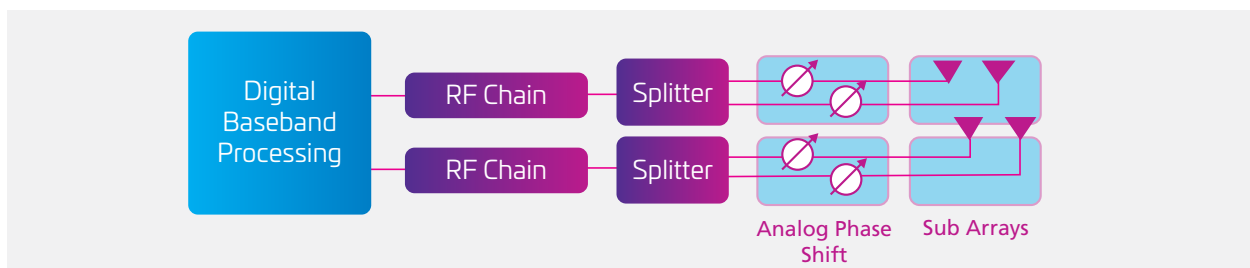


Figure 18: Hybrid beamforming

## Chapter 3: Building a passive beamformer

There is a commonly-held belief that a beamformer must involve active antennas, or antennas with integrated radios. This is not always the case. Passive antennas—when used with 8T8R<sup>††</sup> base station radios [9]—can provide a decent level of electrical beam steering. The result is a beamformer that delivers cost-efficient coverage in low-traffic and suburban areas. The following section discusses the design, performance and use of passive beamformers, specifically those that involve adaptive array antennas.

## Adaptive array antennas (AAA)

### Planar arrays

We have seen how beamforming techniques rely on the alteration of the RF signal phases and amplitudes that are fed across the internal antenna radiating elements. A direct application of this concept is the one-dimensional horizontal or vertical beam steering (e.g., e-tilting) for linear array antennas. To enable a 3D horizontal and vertical beam steering, a two-dimensional rectangular array is needed. This is known as a planar array, a key component of today's adaptive array antennas (AAA).

<sup>††</sup> 8T8R are radios with eight transceivers.

This is our second step in building a practical beamformer.

Adaptive array antennas consist of columns of planar arrays that work together to form a steerable beam that is shaped for improved sidelobes [10]. Adaptive beamforming uses digital signal processing technology to identify the RF signal's direction of arrival (DoA) to a mobile station (MS), and generate a directional beam toward the MS [11].

### Example: CommScope S4 series

The antenna shown in Figure 19 has four x-polarized arrays and each array has two input ports. The antenna is designed for LTE-TDD and 5G NR in 2300–2690 GHz.



Figure 19: A CommScope planer array antenna

### Column pattern and mutual coupling

It should be noted that the horizontal half-power beamwidth (H-HPBW)\*\* listed in planar antenna data sheets is not reflective of the entire panel. Instead, it shows the pattern shape for one of the antenna's four identical columns. The column pattern shape is dependent on a number of physical features. These include the design of the radiating elements, reflector widths and, most importantly, the **inter-column spacing**.

Because an array's behavior is dominated by the mutual coupling between its various elements, the elements generally behave very differently in an array than when isolated [12]. For example, the half-power horizontal beamwidth (HP-HBW) listed on data sheets is inversely affected by column spacing: a 65° HBW typically requires  $0.65\lambda$  spacing between columns, whereas a 90° HBW will use  $0.5\lambda$  spacing. Figure 20 shows this effect for a 7x9 element dipole array ( $\lambda/2$  dipoles,  $\lambda/4$  above ground). Element spacings are denoted as  $D_x$  and  $D_y$ .

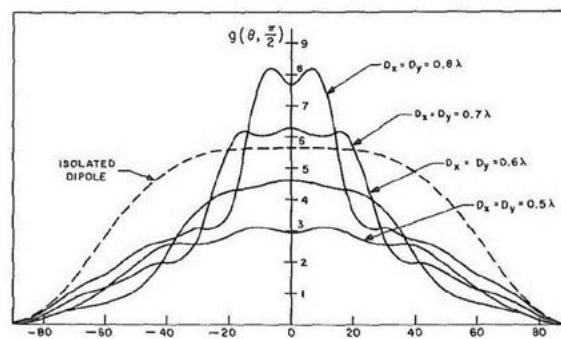


Figure 20: Element spacing vs HP-HBW [12]

\*\* Horizontal half-power beamwidth

## Scanning angle limitations

Depending on its element spacing ( $dx$ ) and steered angle, a linear array with its peak at  $\theta_0$  might create additional large sidelobes (grating lobes). To avoid formation of these lobes, it is important to observe the relationship between the column pattern H-HPBW and the maximum scanning angle. Theory states that, for element spacing  $dx$  ( $0.5\lambda < dx < \lambda$ ), the array factor will have only one single major lobe, and grating-lobe maxima will not occur for  $-90^\circ < \theta_0 < +90^\circ$  as long as  $[13] |\sin\theta_0| > \frac{1}{S} - 1$ , where  $S = dx / \lambda$ .

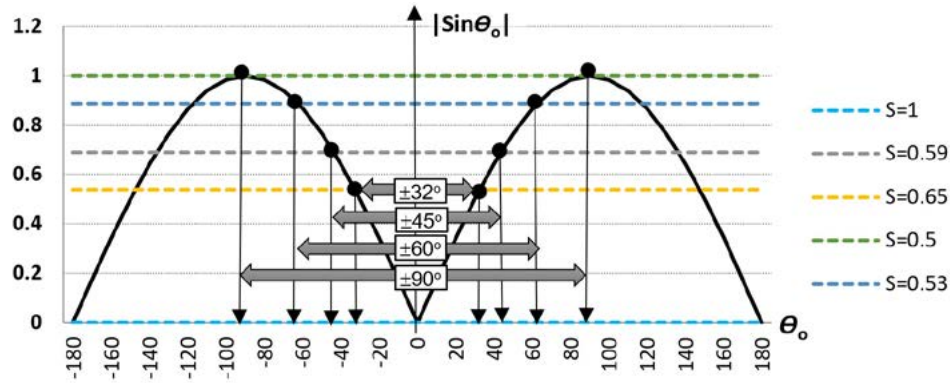


Figure 21: Column spacing vs. max scan angle

In plotting this relationship for different column spacings, as in Figure 21, it is clear that the condition is always true for  $S=0.5$  ( $dx = 0.5\lambda$ ) column spacing, which leads to the maximum  $\pm 90^\circ$  scanning angle range. For max scanning angles of  $\pm 32^\circ$ ,  $\pm 45^\circ$  and  $\pm 60^\circ$ , the spacing is  $0.65\lambda$ ,  $0.59\lambda$  and  $0.53\lambda$ , respectively.

Therefore,  $0.5\lambda$  inter-column spacing corresponds to the  $90^\circ$  column H-HPBW with  $\pm 90^\circ$  antenna scanning angle range. Similarly,  $0.65\lambda$  corresponds to  $65^\circ$  column H-HPBW with  $\pm 32^\circ$  antenna scanning angle range.

## Radiating patterns

Depending on its element spacing ( $dx$ ) and steered angle, a linear array with its peak at  $\theta_0$  might create additional large sidelobes (grating lobes). To avoid formation of these lobes, it is important to observe the relationship between the column pattern H-HPBW and the maximum scanning angle. Theory states that, for element spacing  $dx$  ( $0.5\lambda < dx < \lambda$ ), the array factor will have only one single major lobe, and grating-lobe maxima will not occur for  $-90^\circ < \theta_0 < +90^\circ$  as long as  $[13] |\sin\theta_0| > \frac{1}{S} - 1$ , where  $S = dx / \lambda$ .

An adaptive array beamforming antenna has five main radiating pattern types:

### 1. Single-column pattern

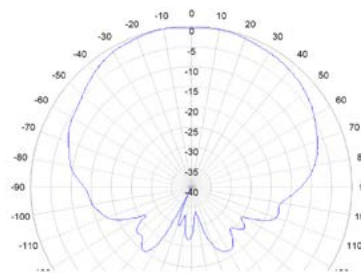


Figure 22: Single-column pattern

This pattern type describes individual arrays in non-beam steering modes. It uses unweighted inputs and is used for uplink channels in some systems.

## 2. Broadcast pattern for LTE

This **wider, non-steerable** beam is intended to cover the entire cell area and is created by feeding four columns with a predesigned set of amplitudes and phases. As the amplitude might be reduced (**tapered**) on some ports for beamforming, a broadcast pattern could exhibit gain reduction, also known as **weighting loss**. This broadcast pattern is usually used for downlink control channels.

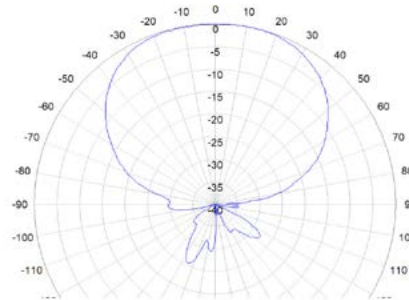


Figure 23: LTE broadcast pattern

## 3. Broadcast pattern for 5G NR

As previously mentioned, unlike LTE, 3GPP defined directional synchronization signals (PSS/SSS/PBCH) for 5G NR. This allows the gNB to sweep its broadcast signal in different directions, using narrower and higher gain beams. While Figure 24 does not represent the traditional radiation pattern plot of a specific antenna, it does capture the envelope for a 5G NR sweeping beam that can be used in planning tools.

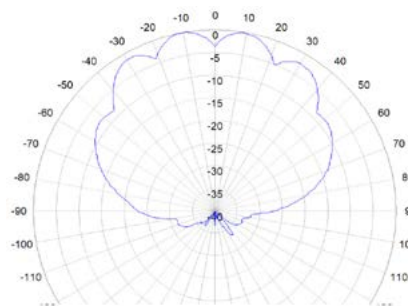


Figure 24: 5G NR broadcast pattern

## 4. Service beam patterns

When all columns are fed together with a uniform phase progression, the result is a **narrow beam that can be steered horizontally**. In a service beam pattern, the amplitudes might be unchanged, or tapered for sidelobe suppression with added weighting losses. In LTE, this type of radiating pattern is used mainly for downlink data traffic.

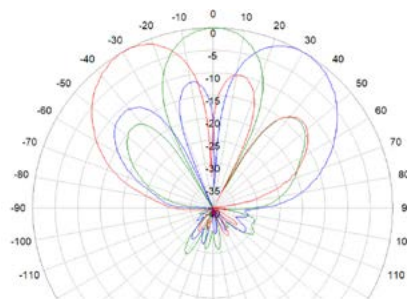


Figure 25: Service pattern

## 5. Soft split patterns

In this mode, the antenna phase and amplitude parameters are set to emulate a twin-beam antenna—three antennas serving six sectors. The result, seen in Figure 26, is two service beams with fixed directions.

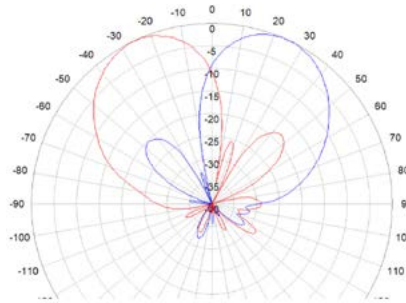


Figure 26: Soft split patterns

## Supporting radios

### Antenna parameters settings

To generate the patterns described above, the 8T8R radios must be able to apply different amplitude and phase shifts across their RF ports. For example, for broadcast or service steering modes, the radios might apply the beam steering settings shown in Table 2. These settings define the phase and amplitude difference for each polarization, across the antennas' four arrays (columns).

| Beam mode          |              | Col 1 | Col 2 | Col 3 | Col 4 |
|--------------------|--------------|-------|-------|-------|-------|
| 65° HBW broadcast  | Phase $\Phi$ | 0     | 115   | 100   | 0     |
|                    | Amplitude    | 0.81  | 1     | 0.73  | 0.6   |
| 90° HBW broadcast  | Phase $\Phi$ | 0     | 130   | 110   | 0     |
|                    | Amplitude    | 0.79  | 1     | 0.75  | 0.6   |
| @0° beam steering  | Phase $\Phi$ | 0     | 0     | 0     | 0     |
|                    | Amplitude    | 1     | 1     | 1     | 1     |
| @30° beam steering | Phase $\Phi$ | 0     | 100   | 200   | 300   |
|                    | Amplitude    | 1     | 1     | 1     | 1     |

Table 2: Example of beam steering settings

## Calibration port

While the settings shown in Table 2 can be accurately applied by the radio, there is no guarantee that the exact values will be received at the antenna's ports. This is especially true given the millimeter variances in the length of the connection jumpers. The calibration port, shown in Figure 27, is designed to compensate for any variance. In the example below, all subarrays are coupled to a single calibration port.

For example, the calibration board shown in Figure 28 utilizes Wilkinson Power dividers that maintain a coupling level of  $-26$  dB between the RF input ports and the calibration port.

The OEM 8T8R radios must also support the calibration functionality. This is done by designing the remote radio unit (RRU) with a dedicated calibration port (Figures 29 and 30) for connection to the corresponding port on the antenna.



Figure 27: Calibration port on a CommScope antenna

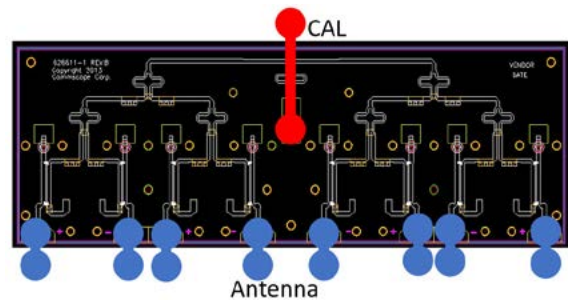


Figure 28: Calibration board

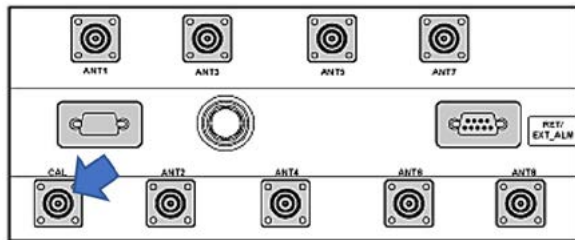


Figure 29: A Huawei TDD LTE RRU3252



Figure 30: Sprint/SAMSUNG 8T8R implementation (U.S.)

## Example: Practical implementation with the AAA

As discussed, having eight RF ports enables the antennas to be deployed in 8T8R TDD mode (eight-branch transmit, eight-branch receive). Beamforming relies on columns with mutual coupling correlations and similar polarizations. As seen in Figure 31, the four cross-polarized columns can be thought of as four co-pol columns on ports 2, 4, 6 and 8 (red) and four cross-pol columns on ports 1, 3, 5 and 7 (blue). In other words, two beamforming antennas (BF1 and BF2) separated by polarization diversity. Depending on the radio, this AAA configuration can support beamforming for modes TM8, 9 and 10 (Table 3) with MIMO schemes of 2x, 8x or multi-user. When configured as in Figure 31—two cross-polarized beamformers with four columns each—the antenna can support 2x MIMO with beamforming.

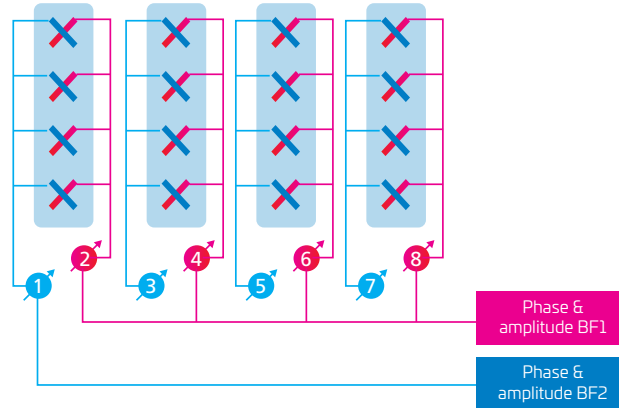


Figure 31: Beamforming with four-column antenna

| Trans. mode | Mapping | Transmission scheme of PDSCH corresponding to PDCCH  | 3GPP release         |
|-------------|---------|--|----------------------|
| TM1         | SISO    | Single-antenna port, port 0                          | Rel. 8               |
| TM2         | MISO    | Transmit diversity                                   | Rel. 8               |
| TM3         | MIMO    | Large delay cyclic delay diversity (CDD)             | Rel. 8               |
| TM4         | MIMO    | Closed-loop spatial multiplexing                     | Rel. 8               |
| TM5         | MIMO    | Multi-user MIMO                                      | Rel. 8               |
| TM6         | MIMO    | Spatial multiplexing using single transmission layer | Rel. 8               |
| TM7         | MIMO    | Single-antenna port                                  | Beamforming, Rel. 8  |
| TM8         | MIMO    | Dual layer transmission                              | Beamforming, Rel. 9  |
| TM9         | MIMO    | Up to 8 layer  | Beamforming, Rel. 10 |
| TM10        | MIMO    | Up to 8 layer  | Beamforming, Rel. 11 |

Table 3: LTE transmission modes for PDCCH and PDSCH configured by C-RNTI (cell-radio network temporary identifier)

## Chapter 4: Building a digital beamformer

Passive beamformers, equipped with up to eight radio transceivers, are capable of dynamic digital horizontal beam steering, vertical analog electrical tilt and 2x2 MIMO streams. But what happens if we increase the radio transceivers beyond eight?

### Massive MIMO concepts

In 2010, Thomas Marzetta of Bell Labs published a paper [14] that considers an **unlimited number** of base station antennas ( $M \rightarrow \infty$ ) serving a fixed number of single-antenna terminals ( $K$ ). This was later described as massive MIMO (mMIMO), a key enabling technology in 5G wireless communications.

Besides the disappearance of uncorrelated noise and fast fading, shown in Marzetta's paper, the use of a large number of mMIMO antenna elements allows narrower, focused and highly directive beams. This improves spectral and energy efficiencies, leading to higher capacities and better cell edge coverage—crucial benefits when considering new 5G spectrum in the 3.5 GHz and mmWave frequency ranges.



Figure 32: The Lund University massive MIMO testbed—(LuMaMi)

But how many antenna elements and transceivers define mMIMO? Usually, that number is around 16T16R and higher. However, as of the writing of this paper, most commercial mMIMO solutions include 32 or 64 transceivers. As the number of RF chains (from transceivers to antenna elements) increases, external jumper cables become impractical. This has led to the integration of radios inside the antenna panels themselves, establishing another breed of beamformers: the so-called active beamformers.

### Massive MIMO dimensioning

To configure mMIMO active beamformers, three factors must be considered:

- Beamforming type
- Transceiver numbers (quantity)
- Antenna element numbers (quantity)

Let's examine each factor closer.

## Beamforming type

The increasing number of antenna elements and RF chains, plus the advent of massive MIMO, pose a number of new challenges [15]:

- Increasing cost and energy consumption caused by the growing number of RF chains—one for each antenna element.
- Determining the channel state information (CSI) between each transmit and receive antenna uses a considerable amount of spectral resources.

One promising solution to these problems is **hybrid beamforming**. Hybrid beamforming uses a combination of **digital beamforming** in the baseband and **analog beamforming** in the RF domain [15].

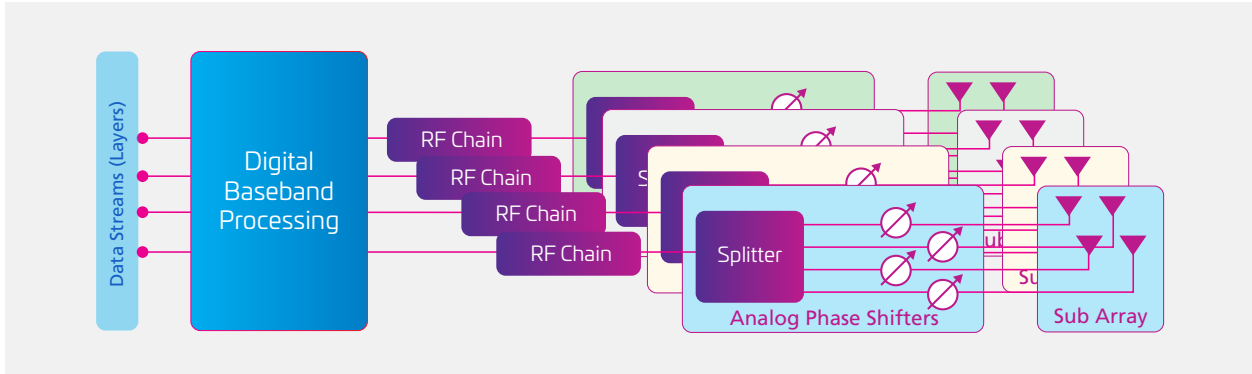


Figure 33: DL hybrid beamforming example

Figure 33 shows a hypothetical example of hybrid beamforming. Each RF chain is digitally controlled and mapped to a single subarray. The RF chain is split across its subarray's antenna elements with analog phase shifters in between.

This configuration might be reduced by removing the analog phase shifters and retaining the subarray's RF splitters. That will increase the antenna panel gain but will not add any analog beamforming capabilities. Such deployments can be usually found in today's sub-6 GHz mMIMO systems and is considered digital (non-hybrid) beamforming.

## Antenna element numbers

As previously mentioned, doubling the number of antenna elements in a lossless linear array reduces the vertical HPBW<sup>§§</sup> and doubles the overall gain.

$$\text{Antenna gain (dB)} = \text{Element gain} + 3\log_2(N)$$

Moreover, a 2D planar array, such as the model shown in Figure 34, can be considered an “array of subarrays.” As such, doubling the number of columns will reduce the horizontal HPBW and further double the overall gain.

§§ Half-power beamwidth

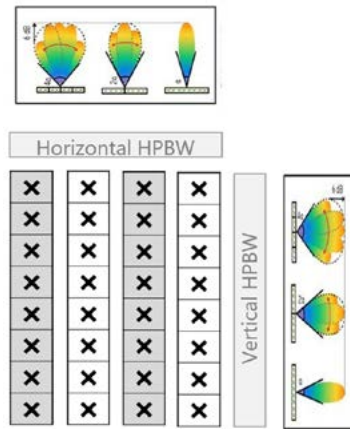


Figure 34: Antenna panel array

To calculate the antenna panel's gain for different mMIMO configurations, assume the above planar array has (H) horizontal subarrays, (V) vertical subarrays and (A) antenna elements in each subarray. If the antenna elements are cross-polarized, then (A) is for a single polarization.

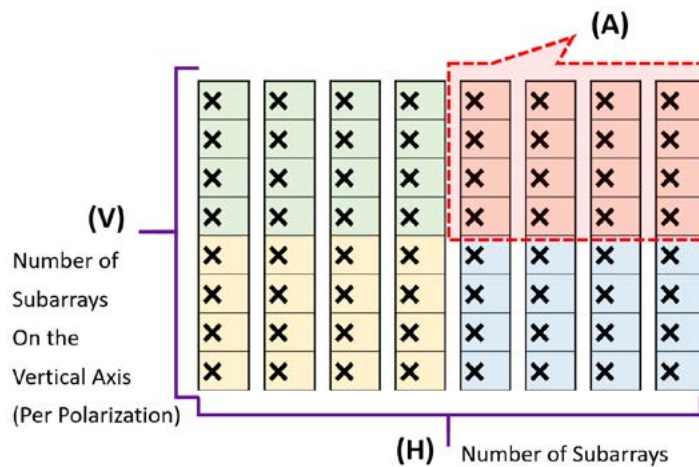


Figure 35: Antenna panel dimensions

To calculate the panel gain from the bottom up, we can use the following:

$$\text{Gain}_{\text{Subarray}} = \text{Gain}_{\text{element}} + 3\log_2(\mathbf{A})$$

$$\text{Gain}_{\text{Panel}} = \text{Gain}_{\text{Subarray}} + 3\log_2(\mathbf{H.V.})$$

Simplifying...

$$\text{Gain}_{\text{Panel}} = \text{Gain}_{\text{element}} + 3\log_2(\mathbf{A}) + 3\log_2(\mathbf{H.V.})$$

$$= \text{Gain}_{\text{element}} + 3\log_2(\mathbf{A.H.V.})$$

$\text{Gain}_{\text{element}}$  is the gain for a single antenna element in front of a back-panel reflector.

To calculate the antenna panel's gain for different mMIMO configurations, assume the above planar array has (H) horizontal subarrays, (V) vertical subarrays and (A) antenna elements in each subarray. If the antenna elements are cross-polarized, then (A) is for a single polarization.

## Transceiver numbers and mapping options

A cross-polarized panel antenna can be thought of as two independent antennas under a single radome, with each polarization independent of the other. A 64T64R radio can then be mapped to 2x 32T32R co-polarized and cross-polarized antennas of identical gains.

Table 4 lists a number of transceivers-to-subarray mapping configurations, for digital (non-hybrid) beamforming. Unless otherwise stated, the table values are for a single polarization.

Looking at Table 4 and Figure 36 below, we can see that each RF chain is always mapped to a single subarray. For example, the first row of Table 4 shows:

- In check sums: an **8T8R** radio consisting of four co-polarized RF chains and four cross-polarized RF chains mapped to 88 co- and cross-polarized antenna elements.
- In panel dimensions: four horizontal by one vertical subarrays. Each subarray has 11 antenna elements.

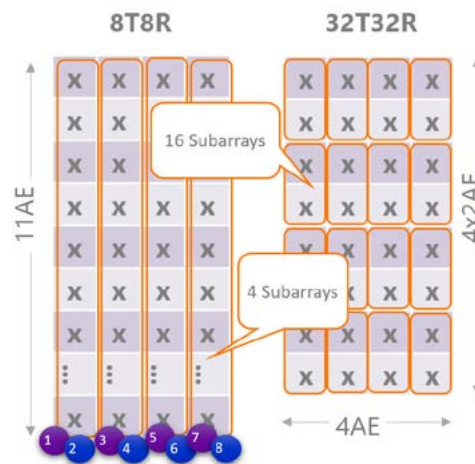


Figure 36: 8T8R and 32T32R mapping

| Panel dimensions  |                 |                 | Check Sums    |                         | Gain Calculations |                  |                             |
|-------------------|-----------------|-----------------|---------------|-------------------------|-------------------|------------------|-----------------------------|
| (H)<br>Horizontal | (V)<br>Vertical | (A)<br>Elements | xTxR<br>Total | Total AE<br>(Dual Pol.) | Ae gain<br>(dBi)  | Subarray<br>Gain | Panel gain<br>(Single Pol.) |
| 4                 | 1               | 11              | 8             | 88                      | 5.1               | 15.48            | 21.48                       |
| 4                 | 4               | 1               | 32            | 32                      | 5.1               | 5.10             | 17.10                       |
| 4                 | 4               | 2               | 32            | 64                      | 5.1               | 8.10             | 20.10                       |
| 4                 | 4               | 4               | 32            | 128                     | 5.1               | 11.10            | 23.10                       |
| 8                 | 2               | 6               | 32            | 192                     | 5.1               | 12.85            | 24.85                       |
| 8                 | 4               | 1               | 64            | 64                      | 5.1               | 5.10             | 20.10                       |
| 8                 | 4               | 2               | 64            | 128                     | 5.1               | 8.10             | 23.10                       |
| 8                 | 4               | 3               | 64            | 192                     | 5.1               | 9.85             | 24.85                       |
| 8                 | 4               | 4               | 64            | 256                     | 5.1               | 11.10            | 26.10                       |

Table 4: Panel gain comparison

In this case, there is one subarray per column ( $V=1$ ). For each polarization, we end up with four subarrays ( $H=4$ ), with each RF chain mapped to an entire column.

RF chains can also be mapped to partial columns, as seen in the third row of Table 4. Here we see:

- A cross-polarized, **32T32R** radio with 16 co-polarized and 16 cross-polarized RF chains
- An antenna with **two antenna elements** per subarray, **four** vertical and **four** horizontal subarrays

This gives us 16 subarrays with each RF chain mapped to one-fourth of a column.

The eighth column of the table compares the resulting panel gains for each configuration, showing that the 8T8R exceeds the 32T32R gain. However, rows 3, 4 and 5 show that, as we increase the number of AEs per subarray—adding more RF chains—we can increase the gain on the 32T32R panel antenna.

## 64T64R AE mapping simulation

Let's consider a 64T64R mMIMO configuration with various options for mapping the cross-polarized planar arrays.

In June 2013, IEEE Communications Magazine cited an interesting study [16], benchmarking several antenna panel configurations. The researchers simulated a network of 19 three-sector cell sites deployed in a hexagonal grid, each site serving 10 UE devices, on average.

Figure 37 illustrates three key panel design parameters used in the simulation:

- A common cross-polarized **64T64R** radio (32 co-polarized and 32 cross-polarized RF chains)
- [1Vx32H]: An antenna of **1AE** per subarray x **1** vertical subarray (V) x **32** horizontal subarrays (H)
- [4Vx8H]: An antenna of **1AE** per subarray x **4** vertical subarrays (V) x **8** horizontal subarrays (H)
  - $0.5\lambda$  horizontal separation ( $d_H$ )
  - $0.5\lambda$  and  $2\lambda$  vertical separation ( $d_V$ )

In the case of a one-dimensional configuration [1Vx32H], such as Figure 38, only horizontal beam steering is possible. However, as the resulting H-HPBW becomes narrower, multiuser interference is reduced to virtually zero. As a result, MU-MIMO with K-user scheduling achieves almost K-times user throughput as the single-user MIMO (SU-MIMO). In this case, K is the number of users in each cell. [16]

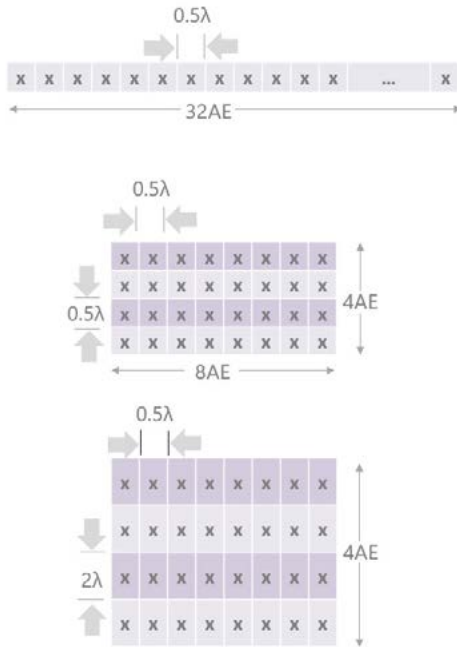


Figure 37: 64T64R mMIMO panel configuration

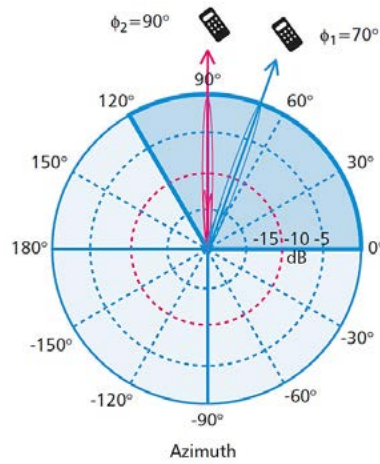


Figure 38: 1Vx32H patterns

Moving into vertical and horizontal beam steering modes with two-dimensional [4Vx8H] panels, both horizontal and vertical beam patterns affect the cell's performance. In the horizontal azimuth, the H-HPBW with 8H elements are now wider than the previous 1D configuration of 32H elements. Yet, there is still sufficient horizontal user segregation across a 120° sector. Note the two users located at 90° and 70° azimuth in Figure 39.

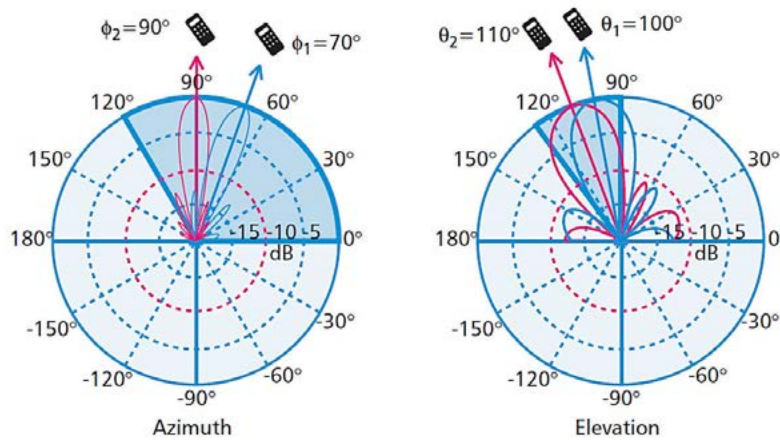


Figure 39: 4Vx8H patterns ( $d_v = 0.5\lambda$ )

However, in the elevation domain with only 4V vertical elements, the V-HPBW is even wider while the vertical spread distribution among users is typically narrower compared to the azimuth. This makes it more difficult to find two UE devices whose beams are sufficiently distinguishable in the vertical elevation domain.

To improve vertical beam discrimination, the authors of the IEEE Communications Magazine study [16] simulated another [4Vx8H] configuration with  $2\lambda$  vertical separation ( $d_v$ ). As shown in Figure 40, this configuration narrows the V-HPBW in the elevation angle range, but also generates several grating lobes, dispersing the energy of the main lobe and causing interference with neighboring cells. This might improve the simulation results for the serving cell but would result in degraded performance across the interfered neighboring cells.

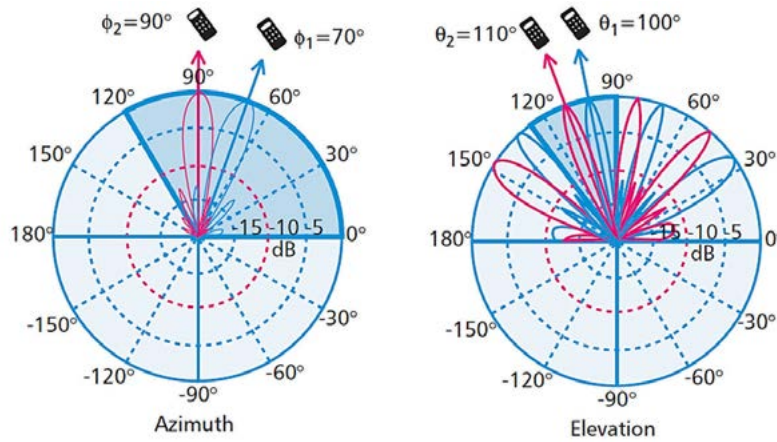


Figure 40: 4Vx8H patterns ( $d_v = 2\lambda$ )

Figure 41 summarizes the spectral efficiency (capacity) for the simulated cell. Capacity is heavily impacted by the horizontal and vertical HPBW. The narrower beams are essential for efficient beam steering and UE discrimination. In most practical scenarios, users are spread across a narrower range of angles in the vertical direction, which limits the benefits and gains of vertical beam steering.

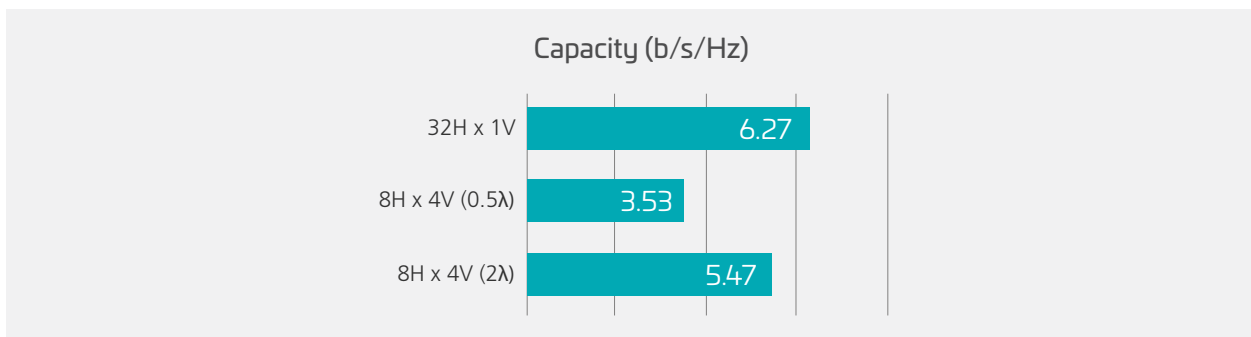


Figure 41: 64T64R performance results [16]

## Conclusion

Now that we are familiar with both passive and active beamformers, one question remains: Can a passive beamformer outperform an active beamformer in the field? In Part II of our analysis, we compare a passive 8T8R beamformer with two active beamformers in 32T32R and 64T64R configurations across three different field environments. Stay tuned to see findings.

## References

- [1] 3GPP, "Study on new radio access technology Physical layer aspects," 3GPP TR 38.802 V14.2.0, 2017.
- [2] M. P. A. R. D. C. a. M. Z. Marco Giordani, "Standalone and Non-Standalone Beam Management for 3GPP NR at mmWaves," IEEE Communications Magazine, April 2019.
- [3] J. Campos, "Understanding the 5G NR Physical Layer," Keysight Technologies 2017, 2017.
- [4] MWC, "White Paper, TM9: Higher Order MIMO Enabler—Maximize Capacity Potential," in MWC, 2018.
- [5] M. Giordani, M. Polese, A. Roy, D. Castor and M. Zorzi, "A Tutorial on Beam Management for 3GPP NR at mmWave Frequencies," IEEE Communications Surveys & Tutorials, vol. 21, no. 1, Q1 2019.
- [6] ShareTechNote, "5G/NR—Beam Management," [Online]. Available: [https://www.sharetechnote.com/html/5G/5G\\_Phys\\_BeamManagement.html](https://www.sharetechnote.com/html/5G/5G_Phys_BeamManagement.html).
- [7] S. J. Orfanidis, Electromagnetic Waves and Antennas, <http://eceweb1.rutgers.edu/~orfanidi/ewa/>, pp. 1110-1111.
- [8] D. A. C. F. A. F. B. G. B. H. J. K. a. E. L. Peter von Butovitsch, "Advanced antenna systems for 5G networks," Ericsson, [Online]. Available: <https://www.ericsson.com/en/reports-and-papers/white-papers/advanced-antenna-systems-for-5g-networks>.
- [9] M. N. Hamdy, "Antenna myths for base station antennas," 2016.
- [10] C. Powell, "Beamforming vs. MIMO antennas," RFS, Meriden, 2014.
- [11] S. S. Q. G. a. X. S. Shanzhi Chen, "Adaptive Beamforming in TDD-Based Mobile Communication Systems: State of the Art and 5G Research Directions," IEEE Wireless Communications, December 2016.
- [12] R. J. Mailloux, Phased Array Antenna Handbook, Artech House, Second Edition.
- [13] T. C. Cheston, Radar Handbook, McGraw Hill, 1990.
- [14] T. L. Marzetta, "Noncooperative Cellular Wireless with Unlimited Numbers of Base Station Antennas," IEEE TRANSACTIONS ON WIRELESS COMMUNICATIONS, vol. VOL. 9, no. NO. 11, NOVEMBER 2010.
- [15] V. V. R. S. H. Z. L. S. L. H. N. L. L. a. K. H. Andreas F. Molisch, "Hybrid Beamforming for Massive MIMO: A Survey," IEEE Communications Magazine, pp. 134-141, 10 2017.
- [16] B. L. N. K. S. Y. L. a. J. (. Z. Y. K. a. J. L. Young-Han Nam, "Full-Dimension MIMO (FD-MIMO) for Next Generation Cellular Technology," IEEE Communications Magazine, pp. 172-179, June 2013.
- [17] K. Benson, "Phased Array Beamforming ICs Simplify," Analog Dialogue, p. 2, 1 1 2019.

CommScope pushes the boundaries of communications technology with game-changing ideas and ground-breaking discoveries that spark profound human achievement. We collaborate with our customers and partners to design, create and build the world's most advanced networks. It is our passion and commitment to identify the next opportunity and realize a better tomorrow. Discover more at [commscope.com](https://commscope.com)

**COMMSCOPE®**

---

[commscope.com](https://commscope.com)

Visit our website or contact your local CommScope representative for more information.

© 2020 CommScope, Inc. All rights reserved.

Unless otherwise noted, all trademarks identified by ® or ™ are registered trademarks or trademarks, respectively, of CommScope, Inc. This document is for planning purposes only and is not intended to modify or supplement any specifications or warranties relating to CommScope products or services. CommScope is committed to the highest standards of business integrity and environmental sustainability, with a number of CommScope's facilities across the globe certified in accordance with international standards, including ISO 9001, TL 9000, and ISO 14001. Further information regarding CommScope's commitment can be found at <https://www.commscope.com/corporate-responsibility-and-sustainability>.

WP-114491-EN (06/00)